blood

Regular Article

HEMATOPOIESIS AND STEM CELLS

The chromatin-binding protein Phf6 restricts the self-renewal of hematopoietic stem cells

Satoru Miyagi,[1,2] Patrycja Sroczynska,[3,4] Yuko Kato,[1,2] Yaeko Nakajima-Takagi,[1] Motohiko Oshima,[1] Ola Rizq,[1] Naoya Takayama,[5] Atsunori Saraya,[1] Seiya Mizuno,[6] Fumihiro Sugiyama,[6] Satoru Takahashi,[6] Yumi Matsuzaki,[2] Jesper Christensen,[3,4] Kristian Helin,[3,4] and Atsushi Iwama[1,7]

[1]Department of Cellular and Molecular Medicine, Graduate School of Medicine, Chiba University, Chiba, Japan; [2]Department of Life Science, Faculty of Medicine, Shimane University, Izumo, Japan; [3]Biotech Research and Innovation Centre (BRIC) and [4]The Novo Nordisk Center for Stem Cell Biology (DanStem), Faculty of Health and Medical Sciences, University of Copenhagen, Copenhagen, Denmark; [5]Department of Regenerative Medicine, Graduate School of Medicine, Chiba University, Chiba, Japan; [6]Laboratory Animal Resource Center, University of Tsukuba, Tsukuba, Japan; and [7]Division of Stem Cell and Molecular Medicine, Center for Stem Cell Biology and Regenerative Medicine, Institute of Medical Science, University of Tokyo, Tokyo, Japan

KEY POINTS

- **Phf6 deficiency augments HSC self-renewal and confers resistance against the TNFα-mediated growth inhibition on HSCs.**

- **Phf6 deficiency alone is not sufficient to induce hematopoietic transformation.**

Recurrent inactivating mutations have been identified in the X-linked plant homeodomain finger protein 6 (*PHF6*) gene, encoding a chromatin-binding transcriptional regulator protein, in various hematological malignancies. However, the role of PHF6 in normal hematopoiesis and its tumor-suppressor function remain largely unknown. We herein generated mice carrying a floxed *Phf6* allele and inactivated *Phf6* in hematopoietic cells at various developmental stages. The *Phf6* deletion in embryos augmented the capacity of hematopoietic stem cells (HSCs) to proliferate in cultures and reconstitute hematopoiesis in recipient mice. The *Phf6* deletion in neonates and adults revealed that cycling HSCs readily acquired an advantage in competitive repopulation upon the *Phf6* deletion, whereas dormant HSCs only did so after serial transplantations. *Phf6*-deficient HSCs maintained an enhanced repopulating capacity during serial transplantations; however, they did not induce any hematological malignancies. Mechanistically, Phf6 directly and indirectly activated downstream effectors in tumor necrosis factor α (TNFα) signaling. The *Phf6* deletion repressed the expression of a set of genes associated with TNFα signaling, thereby conferring resistance against the TNFα-mediated growth inhibition on HSCs. Collectively, these results not only define Phf6 as a novel negative regulator of HSC self-renewal, implicating inactivating *PHF6* mutations in the pathogenesis of hematological malignancies, but also indicate that a *Phf6* deficiency alone is not sufficient to induce hematopoietic transformation. (*Blood*. 2019;133(23):2495-2506)

Introduction

Recent advances have clearly demonstrated the significance of transcriptional regulation by chromatin modifiers in normal hematopoiesis and leukemogenesis. Genomic studies on patients with hematological malignancies have provided insights into a series of mutations in genes considered to be involved in epigenetic gene regulation. These mutations occur in genes known, or suspected, to play a role in modifying the chromatin structure.[1-4] However, it currently remains unclear how many of these genes regulate hematopoiesis under normal conditions and also how mutations in these genes contribute to leukemic transformation and/or progression. This is mainly attributed to the lack of suitable mouse models to evaluate the role of genes in normal hematopoiesis. Knockout mouse models have shown that the loss of *Tet2* or *Dnmt3a*, inactivating mutations that function as driver mutations in human hematological malignancies, confers a growth advantage on hematopoietic stem/progenitor cells,[5-7] thereby contributing to clonal hematopoiesis.

The plant homeodomain (PHD) finger protein 6 (*PHF6*) gene, located on the X chromosome, encodes a chromatin-binding protein with 2 atypical PHD-like zinc finger domains (aPHDs) that has been implicated in transcriptional regulation.[8] Germline mutations in *PHF6* were initially identified in patients with Börjeson-Forssman-Lehmann syndrome, which is characterized by X-linked mental retardation of varying severities,[9] whereas somatic-inactivating mutations frequently occur in patients with T-cell acute lymphoblastic leukemia (T-ALL) and, to a lesser extent, in acute myeloid leukemia (AML), secondary AML, and myelodysplastic syndrome.[10-12] Genome-scale short hairpin RNA (shRNA) screening revealed that the inhibition of *PHF6* expression had a negative impact on the growth of B-cell acute lymphoblastic leukemia (B-ALL) cells, but that it enhanced the tumor progression of AML.[13] These findings indicate that *PHF6* has oncogenic and tumor-suppressive functions in a context-dependent manner.

PHF6 binds to double-stranded DNA in vitro through its aPHD domain and to histone H3 in the absence of DNA. PHF6 has

been reported to bind to a subunit of the nucleosome remodeling and deacetylase (NURD) chromatin-remodeling complex,[14] a component of the transcriptional elongation complex polymerase-associated factor 1 (PAF1),[15] and the transcriptional activator for ribosomal RNA, upstream binding factor 1 (UBF1).[16] Furthermore, integrated genomics revealed that PHF6 binds to nucleosomes surrounding the transcription start site (TSS) of lineage-specific genes and that it modulates the binding of lineage-specific transcription factors.[17] For example, PHF6 binds to the ±1 nucleosome flanking the TSSs of B-cell–specific genes and allows B-cell–specific transcription factors to bind and activate genes in B-ALL cell lines. In contrast, PHF6 binds nucleosomes surrounding the TSSs of T-cell–specific genes and promotes chromatin compaction, thereby restricting the binding of T-cell–specific transcription factors. Thus, these findings provide a model for explaining why the deletion of PHF6 leads to the downregulation of B-cell–specific genes and ectopic activation of the T-cell program in B-ALL cell lines.[17]

To date, despite frequent inactivating mutations in leukemia, limited information is currently available on the role of PHF6 in the hematopoietic system and the characterization of *Phf6* knockout mice has not yet been reported. We generated a mouse line carrying a floxed *Phf6* allele and investigated the role of Phf6 in mouse hematopoietic stem cells (HSCs). We herein demonstrated that Phf6 negatively regulates HSC self-renewal, partly through the activation of genes in tumor necrosis factor α (TNFα) signaling.

Materials and methods

Regarding the conditional deletion of *Phf6*, *Phf6fl/wt* mice were crossed with *Vav1-Cre* (The Jackson Laboratory), *Rosa::Cre-ERT* mice (TaconicArtemis GmbH), or *Mx1-Cre* (The Jackson Laboratory). To induce Cre-ERT activity, mice were injected with 100 μL of tamoxifen dissolved in corn oil at a concentration of 10 mg/mL intraperitoneally for 5 consecutive days. All conditional *Phf6* knockout mice were maintained on a B6-CD45.2 (Japan SLC) genetic background. Polyriboinosinic acid/polyribocytidylic acid (pIpC; InvivoGen) was dissolved in phosphate-buffered saline at a concentration of 4 mg/mL and annealed according to the manufacturer's instructions. To activate the *Mx1-Cre* transgene, adult mice were injected with 400 μg of pIpC 3 times every second day, whereas 3-week-old mice were injected with 160 μg of pIpC once. C57BL/6 mice congenic for the Ly5 locus (B6-CD45.1) were purchased from Sankyo-Laboratory Service (Tsukuba, Japan). Mice were bred and maintained in the Animal Research Facility of the Graduate School of Medicine, Chiba University in accordance with institutional guidelines (approval ID: 29-289).

Results

Generation of mice carrying the *Phf6fl* allele and *Phf6* deletion in hematopoietic cells

To elucidate the biological role of Phf6, we generated mice harboring a *Phf6fl* mutation in which exons 4 and 5 encoding the second aPHD were floxed (Figure 1A), and then crossed *Phf6fl/w* mice with *Vav1-iCre* mice that express *Cre* specifically in hematopoietic cells (*Vav1-iCre;Phf6fl/y*) from the fetal stage. We confirmed the efficient deletion of *Phf6* in CD150+CD34−

lineage marker–negative (Lin−) Sca-1+c-Kit+ (CD150+CD34− LSK) HSCs using quantitative polymerase chain reaction (qPCR) and the western blotting of splenocytes and thymocytes (Figure 1B-C). We hereafter refer to *Vav1-iCre;Phf6wt/y* and *Vav1-iCre; Phf6fl/y* mice as VC and *VC;Phf6Δ/y* mice, respectively. We focused on male mice in the present study because *PHF6* mutations are exclusively found in male patients with AML and T-ALL.[10,11] *VC;Phf6Δ/y* mice were born, grew healthily, and did not exhibit any obvious growth retardation or hypoplasia in their hematopoietic organs at 12 weeks of age (Figure 1D). *VC;Phf6Δ/y* mice had slightly higher white blood cell (WBC) counts than those of the control, which was mainly attributed to increased B lymphopoiesis, whereas they had similar red blood cell counts, hemoglobin levels, and platelet counts (Figure 2A-B). Flow cytometric analyses showed no significant differences in the numbers of long-term HSCs (LT-HSCs), CD34−LSK HSCs, common myeloid progenitors (CMPs), granulocyte-macrophage progenitors (GMPs), megakaryocyte-erythrocyte progenitors (MEPs), and common lymphoid progenitors (CLPs) between VC and *VC;Phf6Δ/y* (Figure 2C; supplemental Figure 1A-C, available on the *Blood* Web site). A cell-cycle analysis using Ki67 expression as a marker for cell proliferation revealed that a significantly higher proportion of *VC;Phf6Δ/y* CD34−LSK HSCs was actively cycling than control cells (Figure 2D). Because the exit of HSCs from the dormant state is often associated with HSC exhaustion, we examined the repopulating capacity of *VC;Phf6Δ/y* HSCs. We transplanted bone marrow (BM) cells from VC or *VC; Phf6Δ/y* CD45.2 male mice together with CD45.1 competitor cells into lethally irradiated CD45.1 recipient mice. The chimerism of *VC;Phf6Δ/y* cells in peripheral blood (PB) CD45+ cells was greater than that of the control in primary (1°) recipients and increased further in secondary (2°) and tertiary (3°) recipients over time (Figure 2E). A lineage distribution analysis 16 weeks after 1°, 2°, and 3° transplantation showed that *VC;Phf6Δ/y* contributed to all 3 hematopoietic lineages more efficiently than VC cells (Figure 2F). The increased chimerism of *VC;Phf6Δ/y* cells was also evident in the HSC fractions (LT-HSCs and CD34−LSK HSCs) and lineage-committed progenitor fractions (GMP and CLP) in 1°, 2°, and 3° recipients (Figure 2G), indicating that the repopulation capacity of *VC;Phf6Δ/y* HSCs was enhanced. Of note, *VC;Phf6Δ/y* HSCs maintained higher chimerism and retained a multilineage differentiation capacity even in 3° transplantation (Figure 2E-G), and did not induce any hematological malignancies (data not shown). We also noted that *VC;Phf6Δ/y* HSCs showed better growth than VC HSCs under HSC culture conditions supplemented with stem cell factor (SCF) and thrombopoietin (TPO). The growth advantage of *VC;Phf6Δ/y* HSCs was completely canceled by retrovirally expressed Phf6 (Figure 2H). These results support a role for Phf6 in the regulation of proliferation. In contrast, the replating capacity of *VC;Phf6Δ/y* LSK hematopoietic stem and progenitor cells under myeloid culture conditions supplemented with SCF, TPO, interleukin-3, and granulocyte macrophage–colony-stimulating factor was similar to that of VC (supplemental Figure 1D).

Phf6 deletion in neonatal and adult hematopoietic cells

To examine the effects of the *Phf6* deletion in neonatal and adult hematopoietic cells, we generated *Mx1-Cre;Phf6fl/y* mice, in which *Mx1* promoter-driven *Cre* expression was induced by injecting pIpC. *Mx1-Cre;Phf6wt/y* and *Mx1-Cre;Phf6fl/y* mice were injected with pIpC at 2 weeks (neonatal stage) or 9 weeks (adult
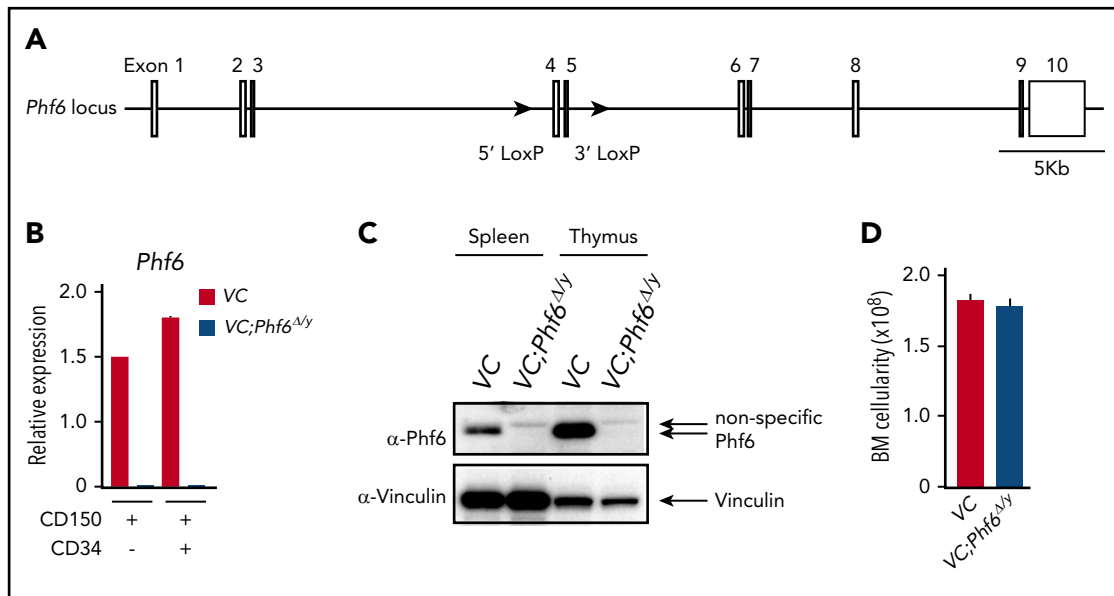
Figure 1. Targeting of the *Phf6* gene in the hematopoietic system. (A) Gene-targeting strategy for the *Phf6* gene. (B) RT-qPCR analysis of *Phf6* in CD150+CD34−LSK HSCs and CD150+CD34+LSK multipotent progenitors. *Hprt1* was used to normalize the amount of input RNA. Data are shown as the mean plus or minus standard error of the mean (SEM) (n = 3). The significance of differences relative to WT is shown. *$P < .05$, **$P < .01$, ***$P < .001$ by the Student *t* test. (C) Western blot analysis of the spleen and thymus. Vinculin was used as a loading control. (D) Total BM cell numbers of the bilateral pairs of femurs and tibiae at 12 weeks of age.

stage) of age, and BM cells were then harvested for competitive transplantation 3 weeks later (Figure 3A). Regardless of the stage of the pIpC injection, genomic qPCR revealed no marked difference in the efficiency of the *Phf6* deletion (pIpC treatment at 2 weeks of age [80.0%] and 9 weeks of age [76.4%]). We hereafter refer to pIpC-treated *Mx1-Cre;Phf6*wt/y* and *Mx1-Cre;Phf6*fl/y* mice as *MC* and *MC;Phf6*Δ/y* mice, respectively. The transplantation of *MC;Phf6*Δ/y* BM cells in which *Phf6* had been deleted for 3 weeks from the neonatal stage gave rise to markedly higher chimerism in all fractions tested than *MC*, whereas the deletion of *Phf6* in the adult stage had a minimal effect and moderately increased chimerism only in myeloid cells and lineage-committed progenitors (GMPs and CLPs), and not in the HSC fractions (Figure 3B-C). The administration of pIpC is known to trigger HSC cycling, which leads to HSC exhaustion in a similar manner to proinflammatory cytokines, such as interferons.[18-20] We found that the chimerism of *MC* cells, which were administrated with pIpC at 2 weeks of age, was reproducibly lower than that of *MC* cells treated with pIpC at 9 weeks of age (Figure 3B-C), indicating that neonatal HSCs, but not adult HSCs, are susceptible to proinflammatory cytokines. Therefore, it is important to note that *VC;Phf6*Δ/y* neonatal HSCs established higher chimerism than that of *MC* neonatal HSCs, indicating that *VC;Phf6*Δ/y* HSCs are more resistant to proinflammatory cytokines. These results together with those obtained from *VC;Phf6*Δ/y* HSCs indicate that the *Phf6* deletion potentiated the repopulating capacity of HSCs more when deleted in embryos or neonates than in adults.

Effects of the *Phf6* deletion on steady-state hematopoiesis

To test the effects of the *Phf6* deletion on steady-state hematopoiesis, we generated *CreERT;Phf6*fl/y* mice in which Cre was activated by injecting tamoxifen. We transplanted whole BM cells from *CreERT;Phf6*wt/y* and *CreERT;Phf6*fl/y* with CD45.1

competitor cells into lethally irradiated CD45.1 recipient mice. After confirming engraftment, we deleted *Phf6* by intraperitoneal injections of tamoxifen 4 weeks after transplantation (Figure 4A). The efficient deletion of *Phf6* was confirmed by genomic PCR on peripheral WBC and the western blotting of peripheral B cells (supplemental Figure 2A-B). We hereafter refer to tamoxifen-treated *CreERT;Phf6*wt/y* and *CreERT;Phf6*fl/y* mice as *CE* and *CE;Phf6*Δ/y* mice, respectively. The tamoxifen injection to recipient mice did not increase the chimerism of *CE;Phf6*Δ/y* cells in PB (Figure 4B-C). In contrast, *CE;Phf6*Δ/y* cells outcompeted CD45.1+ competitor cells in all 3 hematopoietic lineages of PB in 2° recipients (Figure 4B-C). The chimerism of *CE;Phf6*Δ/y* cells also increased in HSCs and progenitor cells in 2° recipients (Figure 4C). These results were in marked contrast to neonatal HSCs, which acquired a competitive advantage immediately after the deletion of Phf6 (Figure 3), and indicate that adult HSCs require long periods of time or hematopoietic stress, such as transplantation, which activates dormant HSCs, to exert an obvious competitive advantage. It is also important to note that 2° recipients reconstituted with *CE;Phf6*Δ/y* cells had mild splenomegaly and increased numbers of LSK cells in the spleen (Figure 4D-F), indicating that *VC;Phf6*Δ/y* HSCs established more active extramedullary hematopoiesis than the control. Consistent with these results, the *Phf6* deletion did not have any significant impact on the proliferation of HSCs in cultures immediately after the deletion (Figure 4G).

Expression profiling of *Phf6*Δ/y* HSCs

To elucidate the molecular mechanisms underlying the enhanced self-renewal capacity of HSCs in the absence of Phf6, we performed RNA sequencing using CD150+CD34−LSK HSCs from 12-week-old *VC* and *VC;Phf6*Δ/y*, 12-week-old *MC* and *MC;Phf6*Δ/y* that had been injected with pIpC at 3 weeks of age, and 1° recipients reconstituted with *CE* or *CE;Phf6*Δ/y* BM cells. BM cells from 12-week-old *MC;Phf6*Δ/y* mice that had been injected
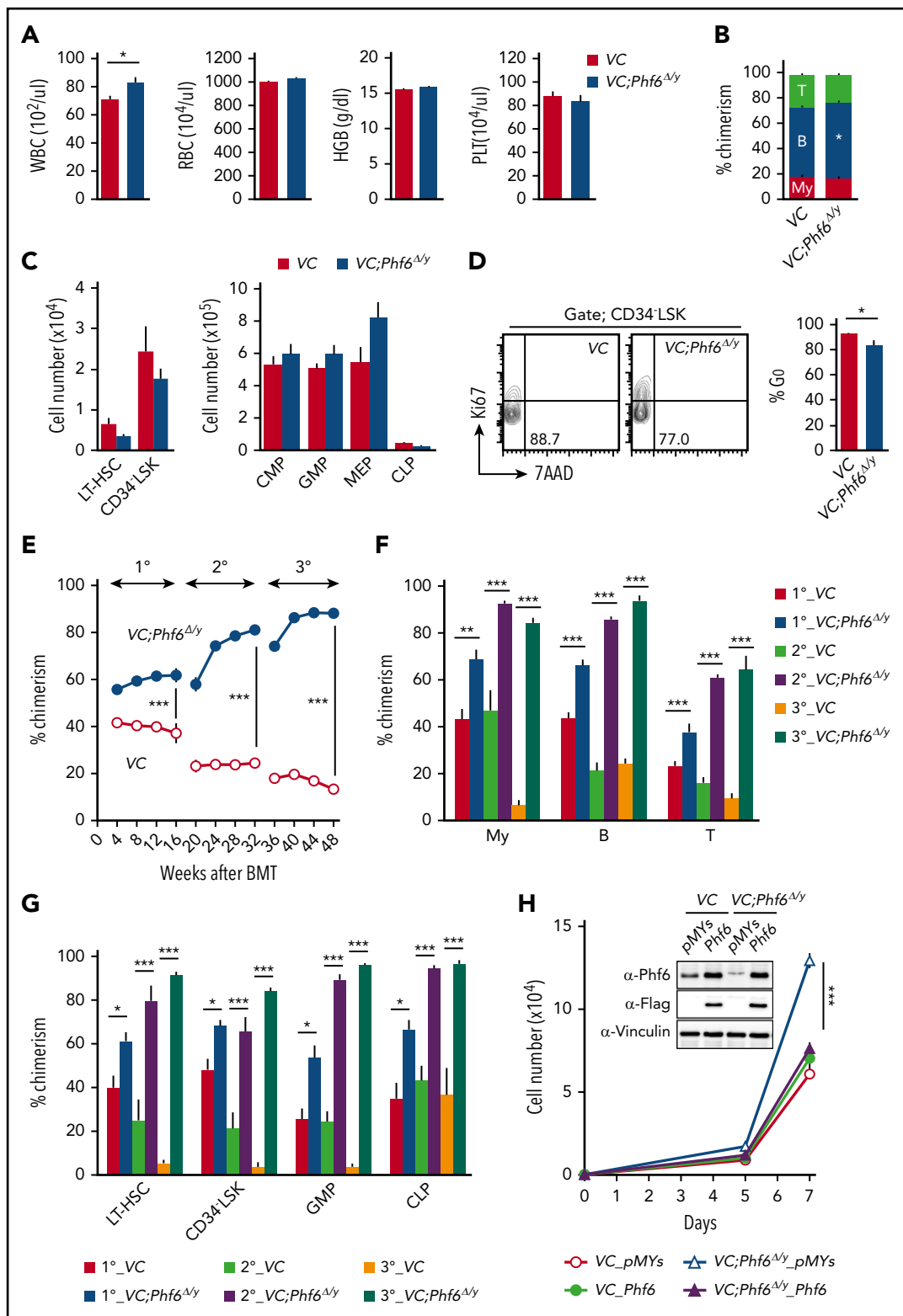
Figure 2. *Phf6* deletion at the fetal stage enhances the repopulating capacity of adult HSCs. (A) PB cell counts in *VC* and *VC;Phf6^Δ/y^* mice. WBC, red blood cell (RBC), and platelet (PLT) counts and hemoglobin (HGB) levels in PB from *VC* (n = 6) and *VC;Phf6^Δ/y^* mice (n = 8) at 12 weeks of age. (B) The proportions of myeloid (My) (Mac-1⁺ and/or Gr-1⁺), B220⁺ B cells, and CD4⁺ or CD8⁺ T cells among CD45.2⁺ cells in PB from *VC* (n = 6) and *VC;Phf6^Δ/y^* (n = 8) mice at 12 weeks of age. (C) Absolute numbers of CD150⁺CD34⁻LSK LT-HSCs, CD34⁻LSK HSCs, myeloid progenitors (CMP, GMP, and MEP), and CLPs in a pool of femurs and tibias from *VC* (n = 5) and *VC;Phf6^Δ/y^* mice (n = 5) at 12 weeks of age. (D) Cell-cycle status of CD34⁻LSK HSCs identified by Ki67 and 7-aminoactinomycin D (7-AAD) staining at 12 weeks of age. Representative flow cytometric profiles (left panel). The proportion of G₀ (Ki67⁻) cells in CD34⁻LSK HSCs is shown as the mean plus or minus SEM (n = 6 or 7) (right panel). (E) Competitive repopulating assays. A total of 5 × 10⁶ BM cells from *VC* and *VC;Phf6^Δ/y^* mice (donor, CD45.2) mixed with the same number of BM cells (competitor, CD45.1) were transplanted into lethally irradiated CD45.1 congenic recipients. In serial transplantations, the same numbers of BM cells from all recipients were pooled and 2 × 10⁶ BM cells were then injected into lethally irradiated CD45.1 congenic recipients. The chimerism of donor-derived CD45.2⁺ cells in the PB of primary (1°), secondary (2°), and tertiary (3°) recipients are shown as the mean
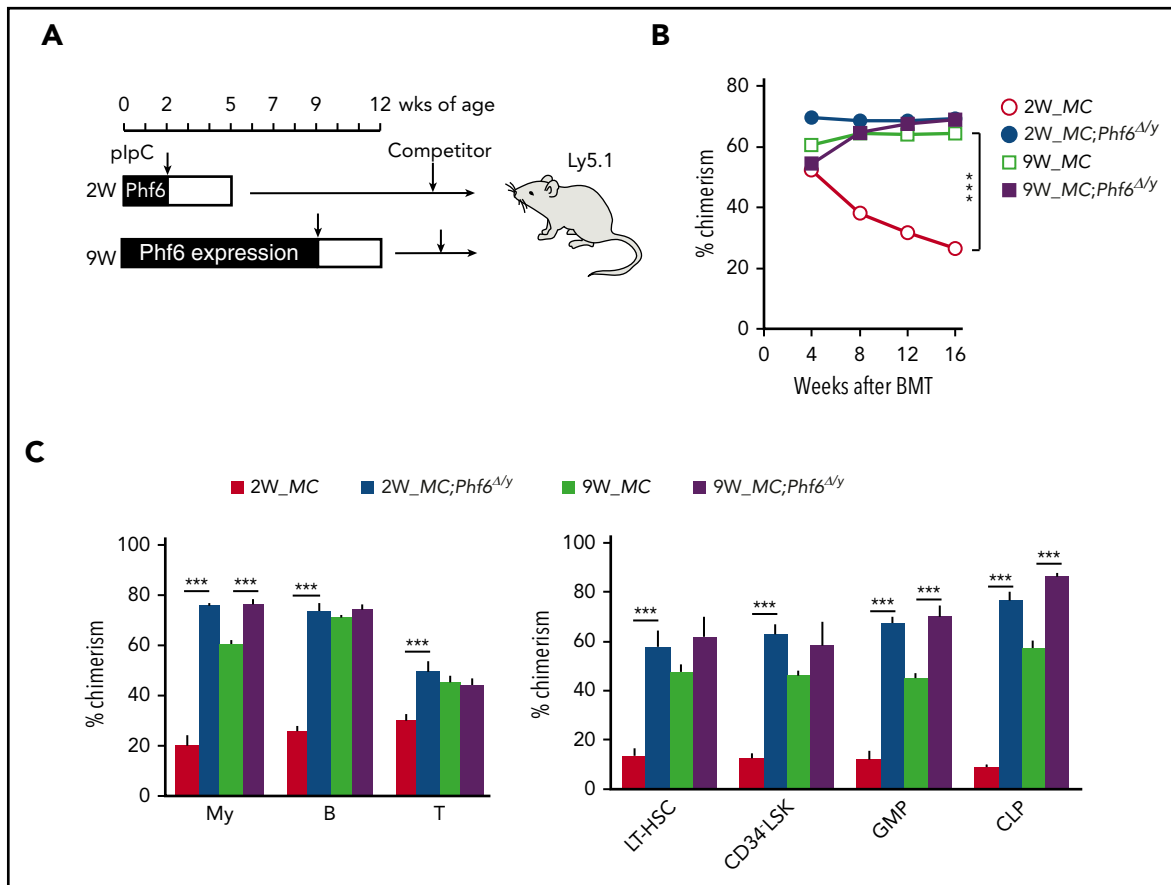
Figure 3. Cycling HSCs are sensitive to the loss of Phf6. (A) Strategy for competitive repopulating assays using the Mx1-Cre system. *Mx1-Cre;Phf6$^{wt/y}$* and *Mx1-Cre;Phf6$^{fl/y}$* mice were injected with pIpC at 2 or 9 weeks of age and BM cells were harvested for competitive transplantation at 5 or 12 weeks of age, respectively. CD45.2 BM cells (5 × 10^6) were transplanted into lethally irradiated CD45.1 recipient mice along with the same number of CD45.1 WT BM cells. (B) The chimerism of CD45.2 donor cells in PB after transplantation (n = 5 or 6). (C) The chimerism of My, B-, and T-cell lineages in PB and those of HSCs and progenitors 16 weeks after transplantation are shown (n = 5 or 6). Data are shown as the mean plus or minus SEM. *$P < .05$, **$P < .01$, ***$P < .001$ by the Student t test.

with pIpC at 7 weeks of age (young adult) also showed an enhanced repopulating capacity (data not shown). Therefore, we also performed RNA sequencing using CD150$^+$CD34$^-$LSK HSCs from 12-week-old *MC* and *MC;Phf6$^{Δ/y}$* that had been injected with pIpC at 7 weeks of age. The results of this analysis revealed that gene-expression profiles were specific to the deleter strain and/or developmental stages of the *Phf6* deletion; for example, only 2 of 296 upregulated genes and 7 of 95 downregulated genes in *VC;Phf6$^{Δ/y}$* HSCs relative to *VC* HSCs were common in these 4 gene sets (supplemental Figure 3A-B), whereas all 4 *Phf6*-deficient HSCs showed similar gene-expression changes in the principal component analysis (supplemental Figure 3C). To identify the gene(s) and/or pathway (s) responsible for the enhanced self-renewal of *Phf6*-deficient HSCs, we divided these data sets into 2 groups according to the *Phf6* genotypes, *Phf6$^{W/y}$* and *Phf6$^{Δ/y}$*, and performed a statistical analysis and gene-set enrichment analysis (GSEA). Seventy-two differentially expressed genes with a q value of <0.05 were identified between *Phf6$^{W/y}$*

and *Phf6$^{Δ/y}$* HSCs (Figure 5A-B) and some of these expression changes were confirmed by reverse transcription (RT)-qPCR (Figure 5C). Sixty-eight of the 72 differentially expressed genes were downregulated in *Phf6$^{Δ/y}$* HSCs, indicating that Phf6 is primarily implicated in transcriptional activation in HSCs; however, Phf6 has been reported to modulate the local chromatin structure in both transcriptionally active and inactive gene promoters.[17] GSEA revealed the positive enrichment of gene sets for E2F targets, MYC targets, and oxidative phosphorylation in *Phf6$^{Δ/y}$* HSCs. In contrast, gene sets for TNFα signaling (which restricts HSC activity),[21] transforming growth factor β signaling (an important niche-associated signaling pathway that maintains HSCs in a dormant state),[22] and the apoptosis pathway were negatively enriched in *Phf6$^{Δ/y}$* HSCs (Figure 5D). These signaling pathways have a negative impact on HSC proliferation and/or survival and may contribute to the unique characteristics of *Phf6*-deficient HSCs, which showed active cell cycling and proliferation. We then investigated the effects of the TNFα treatment on HSC

Figure 2 (continued) plus or minus SEM (n = 5 or 6). (F) The chimerism of My, B-, and T-cell lineages in PB 16, 32, and 48 weeks after 1° transplantation are shown as the mean plus or minus SEM (n = 5 or 6). (G) The chimerism of LT-HSCs, CD34$^-$LSK, GMPs, and CLPs 16, 32, and 48 weeks after 1° transplantation are shown as the mean plus or minus SEM (n = 5 or 6). (H) Growth of *VC* and *VC;Phf6$^{Δ/y}$* CD150$^+$CD34$^-$ LSK HSCs in vitro. Freshly sorted HSCs were transduced with a control retrovirus (*pMYs*) or retrovirus expressing *Phf6* (*Phf6*). After GFP sorting, GFP$^+$ cells were cultured under HSC culture conditions (SCF+TPO) for 7 days. Data are shown as the mean plus or minus SEM of triplicate cultures. Insets, Western blot data of cells in culture on day 7. *$P < .05$, **$P < .01$, ***$P < .001$ by the Student t test. BMT, BM transplantation.
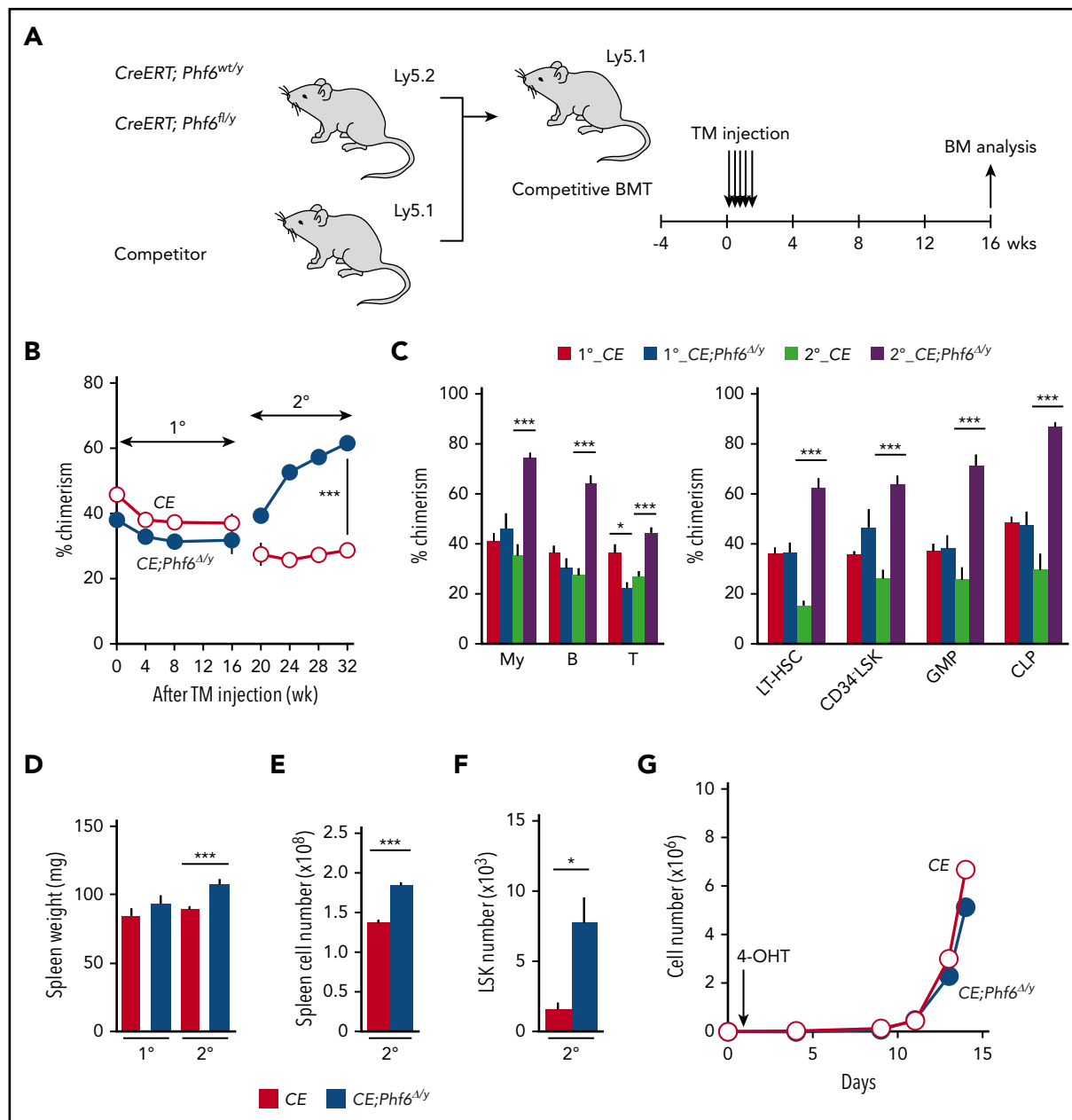
Figure 4. Deletion of *Phf6* in steady-state hematopoiesis. (A) Competitive reconstitution assays using the *CreERT* system. BM cells from 8-week-old *CreERT* and *CreERT; Phf6^fl/y* mice were transplanted into lethally irradiated recipient mice with the same number of competitor BM cells (5 × 10^6 cells). Four weeks after transplantation, recipient mice were injected with tamoxifen (TM) for 5 consecutive days. Serial transplantations were performed as described in Figure 2E. PB analyses were performed every 4 weeks and a BM analysis was performed 16 weeks after the tamoxifen injection. (B) The chimerism of CD45.2^+ donor-derived cells in the PB of recipient mice is shown (n = 5 or 6). (C) The chimerism of My, B-, and T-cell lineages in PB and those of HSCs and progenitors at 16 and 32 weeks after 1° transplantation are shown (n = 5 or 6). (D-F) Spleen weight (D), spleen cell number (E), and the number of LSK cells in the spleen (F) 16 and 32 weeks after 1° transplantation are shown (n = 5). (G) Growth of *CE* and *CE;Phf6^Δ/y* CD150^+CD34^− LSK HSCs in vitro. Freshly sorted HSCs were cultured under HSC culture conditions (SCF+TPO) for 14 days (n = 3). During the culture, cells were treated with 200 nM 4-hydroxytamoxifen (4-OHT) for 16 hours from 24 hours after cell sorting to induce the CreERT-mediated excision of *Phf6*. Data are shown as the mean plus or minus SEM. *P < .05, **P < .01, ***P < .001 by the Student *t* test.

proliferation. *VC;Phf6^Δ/y* HSCs grew significantly better than the control even in the presence of TNFα. The proliferation of *VC* HSCs was inhibited to the same degree by 1 ng/mL TNFα as 20 ng/mL TNFα. In contrast, the same amount of TNFα did not significantly affect the proliferation of *VC;Phf6^Δ/y* HSCs. *VC;Phf6^Δ/y* HSCs proliferated to a similar degree as nontreated *VC* HSCs even in the presence of 5 ng/mL TNFα (Figure 5E). These results indicate that *VC;Phf6^Δ/y* HSCs are significantly more resistant to TNFα-induced growth inhibition than *VC* HSCs

and at least partially explain why the loss of Phf6 confers a competitive advantage on HSCs.

Phf6 activates downstream effectors of TNFα signaling

Fourteen of the 72 differentially expressed genes, such as *Nr4a1*, *Egr1*, and *Junb*, were included in the gene set for TNFα signaling and were downregulated in *Phf6^Δ/y* HSCs (marked as α in
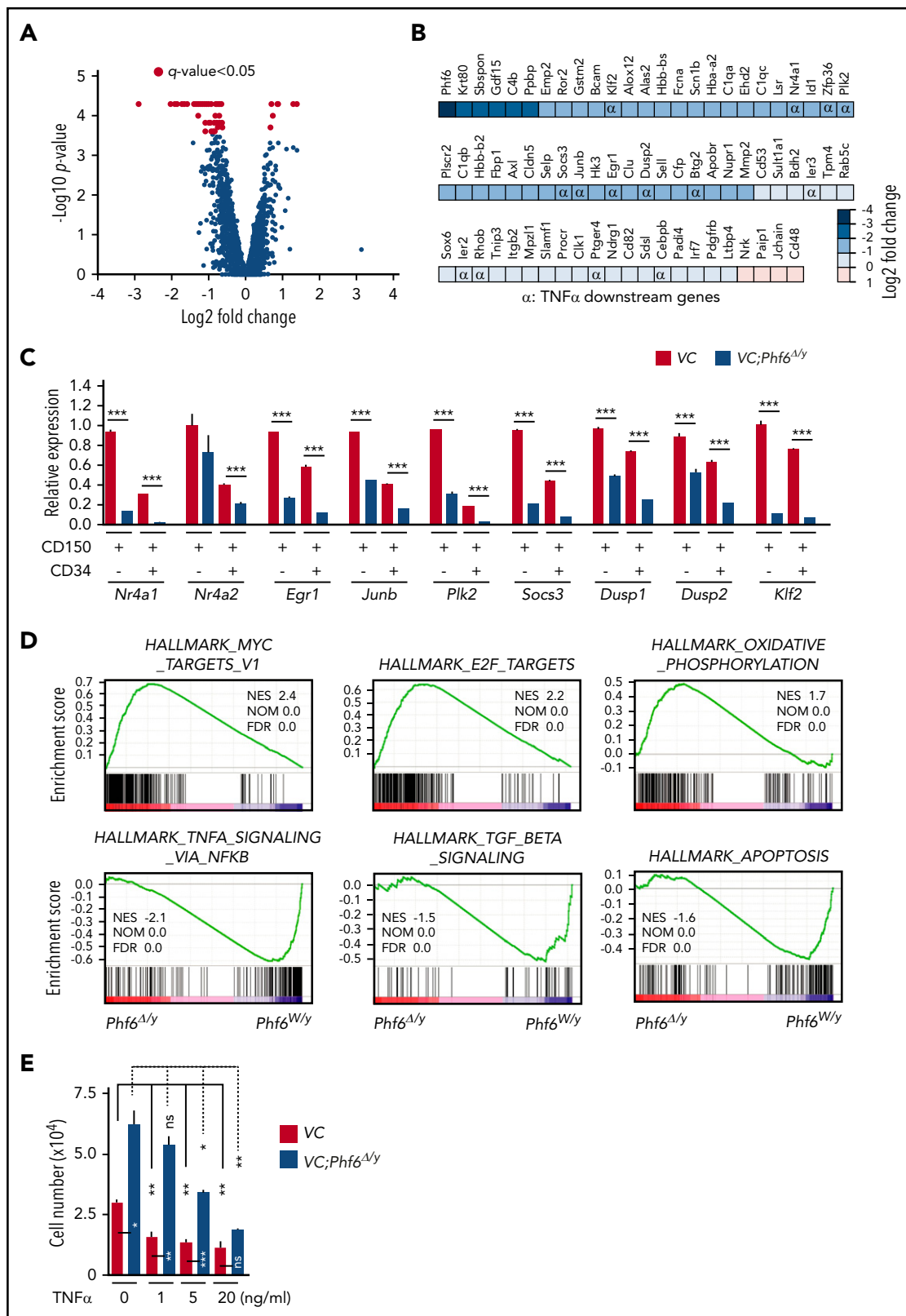
MIYAGI et al

Figure 5. Expression profiling on *Phf6*-deficient HSCs. (A) Volcano plot showing gene-expression changes upon the *Phf6* deletion. Red circles indicate genes that showed significant expression changes (*q* value < 0.05) in *Phf6*$^{\Delta/y}$ HSCs. (B) Differentially expressed genes and their fold-expression changes are shown as a heatmap. "α" shows genes included in the gene set "HALLMARK_TNFA_SIGNALING_VIA_NFKB." (C) RT-qPCR analysis of the indicated genes in CD150+CD34−LSK and CD150+CD34+LSK cells. *Hprt1* was used to normalize the amount of input RNA. Data are shown as the mean plus or minus SEM (n = 3). Significance is shown relative to *VC*. *$P < .05$, **$P < .01$, ***$P < .001$ by the Student *t* test. (D) GSEA performed using RNA-sequence data. GSEA plots of representative data are shown. Normalized enrichment scores (NES), nominal *P* values (NOM), and false discovery rates (FDR) are indicated. (E) Effects of TNFα on HSC proliferation. Freshly sorted HSCs were cultured under HSC culture conditions (10 ng/mL SCF and TPO) with various dosages of TNFα for 10 days. Data are shown as the mean plus or minus SEM. *$P < .05$; **$P < .005$; ***$P < .0005$ by the Student *t* test. TGF, transforming growth factor.
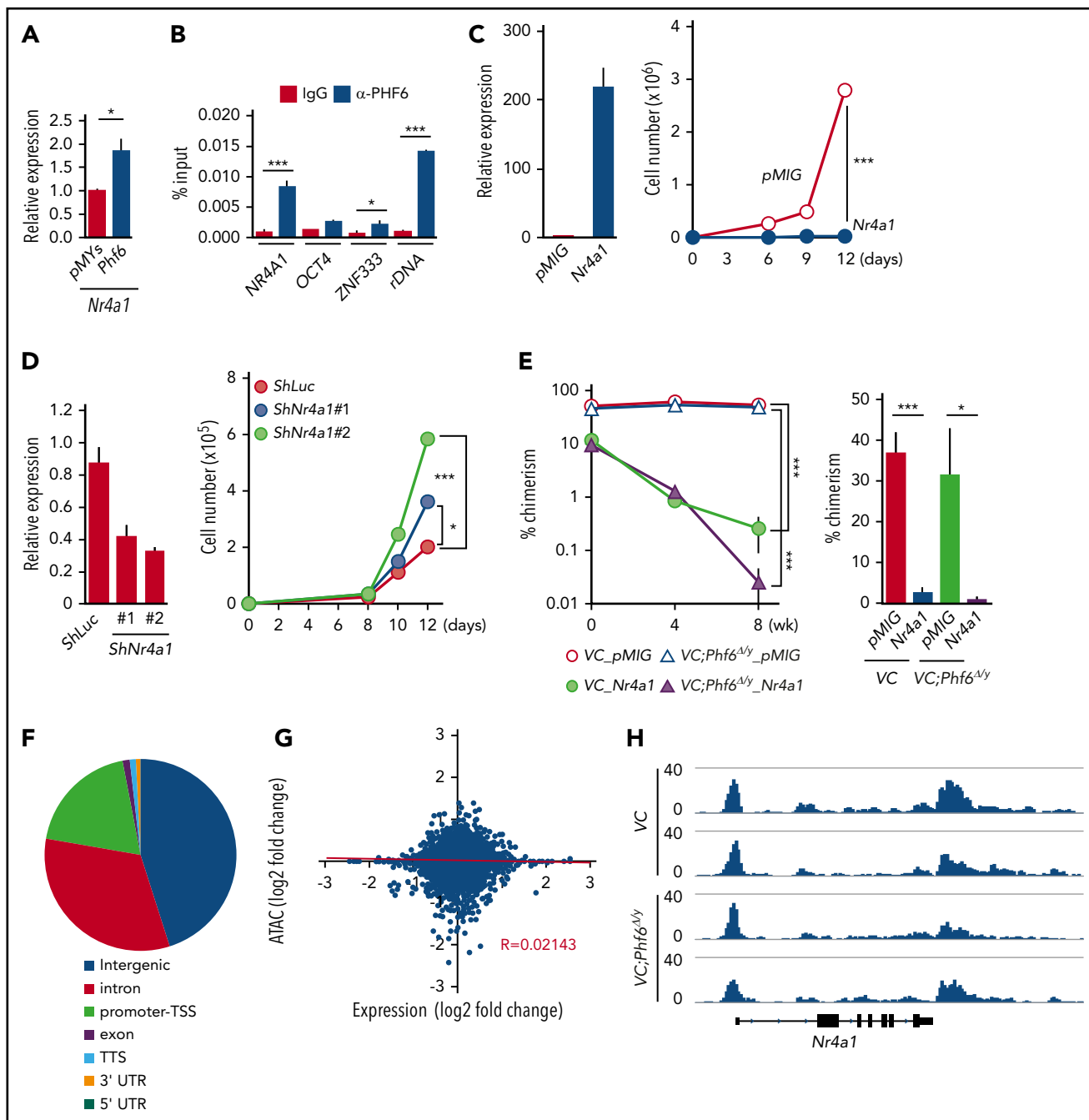
Figure 6. Phf6 activates downstream effectors of TNFα signaling. (A) RT-qPCR analysis of *Nr4a1* in control (*pMYs*) or *Phf6*-transduced LSK cells. (B) ChIP qPCR analysis using the PHF6 antibody in K562 cells. The relative amount of immunoprecipitated DNA is depicted as a percentage of input DNA. Data are shown as the mean plus or minus SEM of triplicate PCRs. Significance is shown relative to the immunoglobulin G (IgG) control. (C) Gain-of-function analysis of the *Nr4a1* gene. HSCs were transduced with a control retrovirus (*pMIG*) or a retrovirus expressing *Nr4a1* (*Nr4a1*). After GFP sorting, GFP+ cells were subjected to a RT-qPCR analysis (left panel) and proliferation assay (right panel). In the proliferation assay, GFP+ cells were cultured under HSC culture conditions (SCF+TPO) for 12 days. (D) Loss-of-function analysis of the *Nr4a1* gene. HSCs were transduced with lentiviruses generating shRNAs against *Luciferase* (*Luc*) or *Nr4a1*, and GFP+ cells were then processed as shown in panel C. (E) Effects of *Nr4a1* expression on *VC;Phf6^Δ/y* HSCs in vivo. HSCs were sorted from *VC* or *VC;Phf6^Δ/y* mice, transduced with a control retrovirus (*pMIG*), or a retrovirus expressing *Nr4a1* (*Nr4a1*), and transplanted into irradiated CD45.1 recipients together with CD45.2 rescue BM cells. The chimerism of GFP+CD45.2+ donor-derived cells in PB (left panel) and BM HSCs 8 weeks after transplantation (right panel) is shown (n = 5 or 6). The chimerism at 0 weeks shows the transduction efficiency of HSCs examined just before transplantation. (F) Pie chart showing the distribution of 75 230 ATAC peaks in HSCs. (G) Scatterplot showing gene-expression changes in *Phf6^Δ/y* HSCs relative to *Phf6^W/y* HSCs and changes in ATAC signals at the proximal promoter regions in *VC;Phf6^Δ/y* HSCs relative to *VC* HSCs. The correlation coefficient between changes in expression and ATAC signals as well as the linear regression are shown in red. (H) Gene tracks showing ATAC peaks in *VC* and *VC;Phf6^Δ/y* HSCs at the *Nr4a1* locus. The x-axis indicates the linear sequence of genomic DNA, and the y-axis represents the total number of mapped reads. rDNA, ribosomal DNA; TTS, transcription termination site; UTR, untranslated region.

Figure 5B). *Nr4a1* is a member of the *Nr4a* family of genes encoding orphan nuclear receptors, including *Nr4a1*, *Nr4a2*, and *Nr4a3*. In contrast to typical nuclear receptors, NR4A subfamily members act as ligand-independent constitutively active transcription factors.[23] *Nr4a1* and *Nr4a3* are tumor-suppressor genes in hematological malignancies and the concomitant deletion
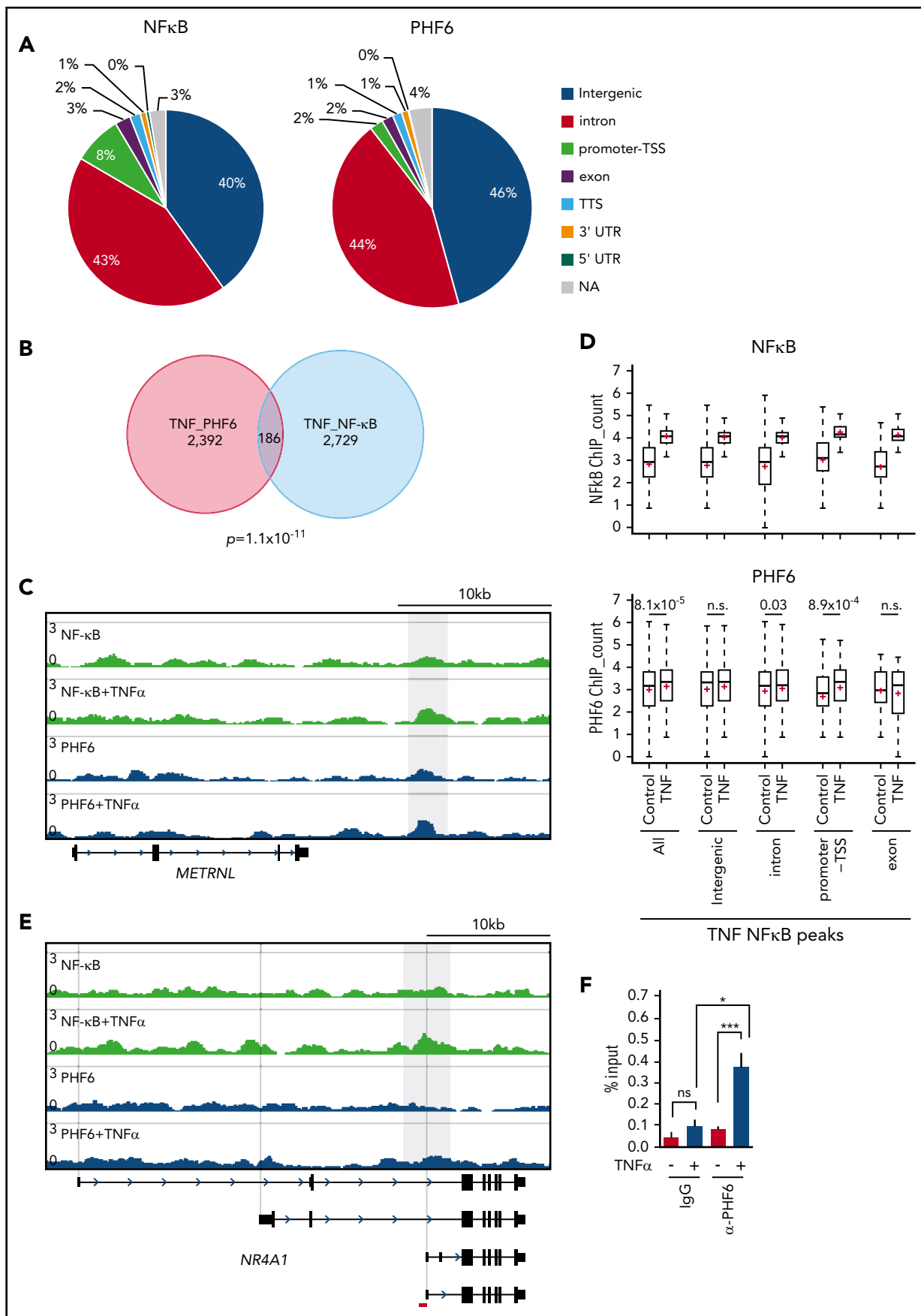
Figure 7.

of *Nr4a1* and *Nr4a3* was previously shown to induce myeloid malignancies associated with the abnormal expansion of LT-HSCs.[24,25] The overexpression of *Nr4a2* has an adverse impact on the repopulating capacity and in vitro proliferation of HSCs by enforcing the quiescence of HSCs.[26] Furthermore, the expression of *Nr4a1* is known to be under the control of TNFα in fibroblasts and dopamine neurons.[27] *Egr1* and *Junb* have also been implicated in the negative regulation of HSC functions,[28,29] and are downregulated in leukemia cells that weakly express *Nr4a*.[25] Collectively, these findings strongly indicate that *Nr4a1* is a target of Phf6 and negatively regulates HSC proliferation, similar to *Nr4a2*, possibly by activating *Egr1* and *Junb* under the control of TNFα. This idea was supported by the results showing that the enforced expression of *Phf6* significantly induced the expression of *Nr4a1* in LSK cells (Figure 6A) and that Phf6 binds to the *NR4A1* promoter in K562 leukemic cells (Figure 6B).

To understand the impact of deregulated *Nr4a1* in *Phf6*[Δ/y] HSCs, we conducted gain- and loss-of-function analyses on *Nr4a1* in HSCs. CD150+CD34−LSK HSCs from wild-type (WT) mice were transduced with an empty or *Nr4a1* virus, sorted according to the expression of green fluorescent protein (GFP) as a marker of transduction, and then cultured for 12 days in media containing SCF and TPO. The enforced expression of *Nr4a1* severely compromised the proliferation of HSCs (Figure 6C), similar to *Nr4a2*.[26] In contrast, the shRNA-mediated knockdown of *Nr4a1* promoted the proliferation of HSCs (Figure 6D). We then investigated the effects of *Nr4a1* overexpression on *VC* and *VC;Phf6*[Δ/y] HSCs in vivo. *VC* or *VC;Phf6*[Δ/y] HSCs were transduced with a control or *Nr4a1* retrovirus and transplanted into lethally irradiated recipients along with Ly5.1 rescue cells. Exogenous *Nr4a1* induced progressive declines in the chimerism of *VC* and *VC;Phf6*[Δ/y] donor cells in PB and HSCs (Figure 6E). These results suggest that the reduced expression of *Nr4a1* at least partially accounts for the enhanced repopulating capacity of *Phf6*[Δ/y] HSCs.

To clarify whether the *Phf6* deletion has any impact on the chromatin configuration in HSCs, we performed an Assay for Transposase Accessible chromatin with high-throughput sequencing (ATAC-Seq) analysis on CD34−LSK HSCs from *VC* and *VC;Phf6*[Δ/y] mice with 2 independent biological replicates. ATAC-Seq profiles open chromatin regions enriched for transcriptional regulatory regions, such as enhancers and promoters. We detected 75 230 peaks after peak calling by counting the peaks in *VC* and *VC;Phf6*[Δ/y] HSCs. These ATAC peaks were mostly located in intergenic regions, promoter TSSs, and introns (Figure 6F). Among them, only 781 and 858 peaks were consistently upregulated (log2 fold change > 1) and downregulated (log2 fold change less than −1), respectively, in 2 *VC;Phf6*[Δ/y] HSC replicates from those in *VC* control HSC replicates. A motif analysis of ATAC peaks in the proximal promoter (TSS ± 2 kb) revealed that only a few DNA motifs were weakly enriched in

VC;Phf6[Δ/y] HSCs (supplemental Figure 3D), whereas none were in *VC* HSCs. We then extracted ATAC peaks in the proximal promoter, compared them with expression profiling data, and found that ATAC signal intensities in proximal promoters positively correlated with the expression levels of genes in *VC* HSCs (supplemental Figure 3E), which supported the validity of ATAC-Seq data. However, no correlation was observed between fold changes in gene expression and ATAC signals in *VC;Phf6*[Δ/y] HSCs relative to *VC* HSCs (Figure 6G). For example, the ATAC signal was similarly observed at the *Nr4a1* promoter in *VC* and *VC;Phf6*[Δ/y] HSCs (Figure 6H), even though the expression of *Nr4a1* had clearly decreased in *VC;Phf6*[Δ/y] HSCs. These results demonstrate that the *Phf6* deletion had a minimal effect on the chromatin configuration, suggesting that Phf6 regulates transcriptional activation at the step after chromatin relaxation around transcriptional regulatory elements.

PHF6 has been reported to bind to gene bodies and proximal promoter/enhancer regions of many annotated genes, where it modulates the binding or activity of lineage-specific transcription factors.[17] The binding motifs of NF-κB, an important downstream effector in the TNFα signaling pathway, were enriched in PHF6-bound DNA fragments.[17] Physical interaction of PHF6 with NF-κB has also been reported.[17] These results imply that PHF6 physically interacts with transcription factors, such as NF-κB, and augments their capacity to activate transcription. However, we could not reproduce the physical interaction between PHF6 and NF-κB (p65) in TNFα-treated K562 cells (data not shown). We then performed chromatin immunoprecipitation (ChIP) combined with high-throughput sequencing of PHF6 and NF-κB (p65) using K562 cells treated with TNFα. PHF6 and NF-κB peaks were mainly detected in the intergenic regions, introns, and promoter TSSs (Figure 7A). The average sizes for the PHF6 and NF-κB peaks were 162 bp and 223 bp, respectively. Of note, PHF6 and NF-κB peaks significantly overlapped in K562 cells treated with TNFα (Figure 7B-C). NF-κB signals were markedly enhanced in all genomic regions upon TNFα treatment, whereas PHF6 signals in these NF-κB–bound regions were moderately albeit significantly enhanced in the promoter TSSs regions and, to a lesser extent, in introns (Figure 7D). These observations strongly indicate the functional interaction between PHF6 and NF-κB. When we checked the colocalization of the PHF6 and NF-κB peaks within 100 bp upstream and downstream of each peak, an additional 52 peaks appeared to be in close proximity to each other, suggesting that PHF6 also facilitates p65 binding in an indirect way via changing the chromatin accessibility in the locus.

Among 68 of the 72 differentially expressed genes downregulated in *Phf6*[Δ/y] HSCs, only 11 genes (*Gstm2*, *Klf2*, *Fbp1*, *Cd82*, *Mpzl1*, *Sox6*, *Cd53*, *Cldn5*, *Ptger4*, *Ror2*, and *Selp*) appeared to be the direct targets of PHF6 in K562 cells. Although the peak calling failed to identify PHF6 peaks at the *NR4A1* locus, TNFα

Figure 7. TNFα enhances the genomic binding of PHF6. (A) Pie chart showing the distribution of PHF6 and NF-κB (p65) peaks. (B) Venn diagram showing the overlap between PHF6 and NF-κB (p65) peaks. (C) Gene tracks showing PHF6 and NF-κB (p65) peaks in control and TNFα-treated K562 cells at the *METRNL* locus. The x-axis indicates the linear sequence of genomic DNA, and the y-axis represents the total number of mapped reads. (D) Box-and-whisker plots showing NF-κB (p65) and PHF6 ChIP combined with high-throughput sequencing signals in the NF-κB–bound regions identified in TNFα-treated K562 cells. Boxes represent 25 to 75 percentile ranges. Vertical lines represent 10 to 90 percentile ranges. Horizontal bars represent medians. Mean values are indicated by red crosses. (E) Gene tracks showing PHF6 and NF-κB (p65) peaks in control and TNFα-treated K562 cells at the *NR4A1* locus. The x-axis indicates the linear sequence of genomic DNA, and the y-axis represents the total number of mapped reads. The region detected by ChIP qPCR is indicated by a red bar. (F) ChIP qPCR assays for NF-κB (p65) and PHF6 in control and TNFα-treated K562 cells at the *NR4A1* locus. The relative amounts of immunoprecipitated DNA are depicted as percentages of input DNA. Data are shown as the mean plus or minus SEM of triplicate PCRs. *P < .05, **P < .01, ***P < .001 by the Student *t* test. NA, not applicable; n.s., not significant.

enhanced binding of PHF6 to the region encompassing introns 3 and 4 of *NR4A1*, in which the ENCODE project identified the peak of acetylated histone H3 at lysine 27 (https://genome.ucsc.edu) (Figure 7E). This observation was validated by ChIP qPCR (Figure 7F). These results indicate that PHF6 regulates expression of the downstream effector genes of TNFα signaling at the step after chromatin relaxation around transcriptional regulatory elements, by modulating the function of transcription factors, such as NF-κB.

Discussion

In the present study, we demonstrated that *Phf6* is a critical negative regulator of HSC self-renewal. The loss of Phf6 potentiated the repopulating capacity of adult HSCs independently of the developmental stages of the *Phf6* deletion. However, we observed a marked difference in kinetics; neonatal HSCs acquired a competitive advantage immediately after the loss of Phf6, whereas adult HSCs required a longer time period or hematopoietic stress, such as secondary transplantation, indicating that actively cycling HSCs are more sensitive to the *Phf6* deletion than dormant HSCs. In the S phase of the cell cycle, chromatin undergoes transient disruption and restoration to replicate parental chromatin. During the restoration process, parental nucleosomes containing histone marks are diluted by the deposition of newly synthesized histones. Thus, chromatin replication is a time window of opportunity for changing the chromatin structure, thereby altering the transcription factor profile on chromatin.[30] A proteomic analysis identified PHF6 as a component of nascent chromatin.[31] These findings implicate PHF6 in the loading of transcription factors on chromatin or the functional regulation of transcription factors in the S phase. This may explain why cycling HSCs acquired enhanced repopulating activity in a shorter time than dormant HSCs upon *Phf6* deletion. Of note, the CRISPR/Cas9-mediated deletion of *Phf6* did not affect the proliferation of ES cells or leukemic cell lines (S. Miyagi, unpublished data), indicating that Phf6 is not a general negative regulator of cell-cycle progression, but functions in a cell-context–dependent manner. The *Phf6* deletion led to the downregulation of a set of genes associated with TNFα signaling and conferred resistance against the TNFα-mediated growth inhibition on HSCs by directly and indirectly activating the downstream effectors of TNFα signaling, such as *Nr4a1*, *Egr1*, and *Junb*. TNFα is induced by hematopoietic stress, such as total-body irradiation, infection, and inflammation. Correspondingly, a previous study demonstrated that the deletion of genes encoding receptors for TNFα, *Tnfrsf1a* and *Tnfrsf1b*, enhanced the repopulating capacity of HSCs without affecting the HSC pool size in donor mice after transplantation[21]; however, the role for TNFα in steady-state hematopoiesis remains controversial. Therefore, the impact of Phf6 loss may become more apparent under stress conditions, such as transplantation, but not under steady-state conditions.

Recurrent inactivating mutations have been identified in the X-linked *PHF6* gene in various hematological malignancies. Consistent with this, *Phf6*^Δ/y HSCs showed better chimerism than control HSCs in a competitive setting, which was maintained in the long-term in a serial transplantation setting, indicating that a *Phf6* deficiency promotes HSC self-renewal. The expression and secretion of inflammatory cytokines, such as TNFα and interleukin-6 (which are inhibitory toward normal HSCs),[32-34] are deregulated in hematological malignancies, including myelodysplastic syndrome and AML. These findings together with the present results showing

that the loss of Phf6 confers resistance to TNFα on HSCs suggest a role for inactivating mutations in *PHF6* in promoting the transformation and clonal evolution of hematopoietic cells. Because cycling HSCs readily acquired a growth advantage over dormant HSCs by the loss of Phf6, a *PHF6* insufficiency in infants and young children may have a stronger impact on the pathogenesis of hematological malignancies than in adults. *PHF6* has been identified as the second most frequently mutated gene in pediatric cancers.[35] However, *VC;Phf6*^Δ/y HSCs retained a multilineage differentiation capacity during serial transplantations and did not induce any hematological malignancies, even in 3° recipient mice. These findings indicate that a *Phf6* insufficiency alone is not adequate to induce hematopoietic transformation; cooperating mutations are needed. This idea is supported by the overexpression of microRNA targeting *Phf6* accelerating the onset of leukemia in Notch1-induced T-ALL in mice.[36] In this regard, it will be interesting to examine whether the deletion of *Phf6* accelerates the development of AML induced by *RUNX1* mutants because *RUNX1* mutations significantly co-occur with *PHF6* mutations in patients with myeloid malignancies.[12]

HSCs from *VC;Phf6*^Δ/y male mice showed an enhanced repopulating capacity; therefore, HSCs from *VC;Phf6*^Δ/Δ females and *VC;Phf6*^Δ/wt females with inactivated WT X chromosomes are considered to acquire an enhanced repopulating capacity in a similar manner to HSCs from *Phf6*^Δ/y males. Although *PHF6* mutations are highly male biased in AML and T-ALL,[10,11] it will also be interesting to investigate the phenotypes of HSCs from *VC;Phf6*^Δ/wt and *VC;Phf6*^Δ/Δ female mice.

During the preparation of our revised manuscript, Wendorff et al reported that the *Phf6* deletion using *Vav1-iCre* and *CreERT* deleter lines enhances self-renewal of HSCs in a setting of serial transplantation.[37] Their findings are consistent with ours. However, there are several differences in profiles of altered gene expression and chromatin accessibility upon the deletion of *Phf6*. Wendorff et al performed these analyses using the *CreERT2* deleter, whereas we used the *Vav1-iCre* deleter. We speculate that the discrepancies are mainly attributed to the deleter strains and the developmental stages of *Phf6* deletion. As we showed in the present study, the expression profiles of HSCs upon the deletion of *Phf6* are greatly affected by these factors.

Authorship

Contribution: S. Miyagi, J.C., K.H., and A.I. designed this study; S. Miyagi performed experiments, analyzed data, and actively wrote the manuscript; P.S., Y.K., Y.N.-T., O.R., Y.M., and N.T. performed experiments and analyzed data; M.O. analyzed next-generation sequencing data; A.S., S. Mizuno, F.S.,

and S.T. generated the *Phf6* knockout mouse; and K.H. and A.I. conceived of and directed the project, secured funding, and actively wrote the manuscript.

Conflict-of-interest disclosure: The authors declare no competing financial interests.

ORCID profile: A.I., 0000-0001-9410-8992.

Correspondence: Satoru Miyagi, Department of Life Science, Faculty of Medicine, Shimane University, 89-1 Enya, Izumo City, Shimane 693-8501, Japan; e-mail: miyagi@med.shimane-u.ac.jp; Kristian Helin, Biotech Research and Innovation Centre (BRIC), University of Copenhagen, Ole Maaløes Vej 5, 2200 Copenhagen, Denmark; e-mail: helink@mskcc.org; or Atsushi Iwama, Department of Cellular and Molecular Medicine, Graduate School of Medicine, Chiba University, 1-8-1 Inohana, Chuo-ku, Chiba 260-8670, Japan; e-mail: 03aiwama@ims.u-tokyo.ac.jp.

Footnotes

REFERENCES

1. Belver L, Ferrando A. The genetics and mechanisms of T cell acute lymphoblastic leukaemia. *Nat Rev Cancer.* 2016;16(8):494-507.

2. Bowman RL, Busque L, Levine RL. Clonal hematopoiesis and evolution to hematopoietic malignancies. *Cell Stem Cell.* 2018;22(2):157-170.

3. Chen SJ, Shen Y, Chen Z. A panoramic view of acute myeloid leukemia. *Nat Genet.* 2013; 45(6):586-587.

4. Cancer Genome Atlas Research Network; Ley TJ, Miller C, Ding L, et al. Genomic and epigenomic landscapes of adult de novo acute myeloid leukemia. *N Engl J Med.* 2013; 368(22):2059-2074.

5. Challen GA, Sun D, Jeong M, et al. Dnmt3a is essential for hematopoietic stem cell differentiation. *Nat Genet.* 2011;44(1):23-31.

6. Ko M, Bandukwala HS, An J, et al. Ten-eleven-translocation 2 (TET2) negatively regulates homeostasis and differentiation of hematopoietic stem cells in mice. *Proc Natl Acad Sci USA.* 2011;108(35):14566-14571.

7. Moran-Crusio K, Reavie L, Shih A, et al. Tet2 loss leads to increased hematopoietic stem cell self-renewal and myeloid transformation. *Cancer Cell.* 2011;20(1):11-24.

8. Todd MA, Ivanochko D, Picketts DJ. PHF6 degrees of separation: the multifaceted roles of a chromatin adaptor protein. *Genes (Basel).* 2015;6(2):325-352.

9. Lower KM, Turner G, Kerr BA, et al. Mutations in PHF6 are associated with Börjeson-Forssman-Lehmann syndrome. *Nat Genet.* 2002;32(4):661-665.

10. Van Vlierberghe P, Palomero T, Khiabanian H, et al. PHF6 mutations in T-cell acute lymphoblastic leukemia. *Nat Genet.* 2010;42(4):338-342.

11. Van Vlierberghe P, Patel J, Abdel-Wahab O, et al. PHF6 mutations in adult acute myeloid leukemia. *Leukemia.* 2011;25(1):130-134.

12. Mori T, Nagata Y, Makishima H, et al. Somatic PHF6 mutations in 1760 cases with various myeloid neoplasms. *Leukemia.* 2016;30(11):2270-2273.

13. Meacham CE, Lawton LN, Soto-Feliciano YM, et al. A genome-scale in vivo loss-of-function screen identifies Phf6 as a lineage-specific regulator of leukemia cell growth. *Genes Dev.* 2015;29(5):483-488.

14. Todd MA, Picketts DJ. PHF6 interacts with the nucleosome remodeling and deacetylation (NuRD) complex. *J Proteome Res.* 2012;11(8):4326-4337.

15. Zhang C, Mejia LA, Huang J, et al. The X-linked intellectual disability protein PHF6 associates with the PAF1 complex and regulates neuronal migration in the mammalian brain. *Neuron.* 2013;78(6):986-993.

16. Wang J, Leung JW, Gong Z, Feng L, Shi X, Chen J. PHF6 regulates cell cycle progression by suppressing ribosomal RNA synthesis. *J Biol Chem.* 2013;288(5):3174-3183.

17. Soto-Feliciano YM, Bartlebaugh JME, Liu Y, et al. PHF6 regulates phenotypic plasticity through chromatin organization within lineage-specific genes. *Genes Dev.* 2017;31(10):973-989.

18. Sato T, Onai N, Yoshihara H, Arai F, Suda T, Ohteki T. Interferon regulatory factor-2 protects quiescent hematopoietic stem cells from type I interferon-dependent exhaustion. *Nat Med.* 2009;15(6):696-700.

19. Baldridge MT, King KY, Boles NC, Weksberg DC, Goodell MA. Quiescent haematopoietic stem cells are activated by IFN-gamma in response to chronic infection. *Nature.* 2010; 465(7299):793-797.

20. Essers MA, Offner S, Blanco-Bose WE, et al. IFNalpha activates dormant haematopoietic stem cells in vivo. *Nature.* 2009;458(7240):904-908.

21. Pronk CJ, Veiby OP, Bryder D, Jacobsen SE. Tumor necrosis factor restricts hematopoietic stem cell activity in mice: involvement of two distinct receptors. *J Exp Med.* 2011;208(8):1563-1570.

22. Yamazaki S, Iwama A, Takayanagi S, Eto K, Ema H, Nakauchi H. TGF-beta as a candidate bone marrow niche signal to induce hematopoietic stem cell hibernation. *Blood.* 2009; 113(6):1250-1256.

23. Wang Z, Benoit G, Liu J, et al. Structure and function of Nurr1 identifies a class of ligand-independent nuclear receptors. *Nature.* 2003;423(6939):555-560.

24. Mullican SE, Zhang S, Konopleva M, et al. Abrogation of nuclear receptors Nr4a3 and Nr4a1 leads to development of acute myeloid leukemia. *Nat Med.* 2007;13(6):730-735.

25. Ramirez-Herrick AM, Mullican SE, Sheehan AM, Conneely OM. Reduced NR4A gene dosage leads to mixed myelodysplastic/myeloproliferative neoplasms in mice. *Blood.* 2011;117(9):2681-2690.

26. Sirin O, Lukov GL, Mao R, Conneely OM, Goodell MA. The orphan nuclear receptor Nurr1 restricts the proliferation of haematopoietic stem cells. *Nat Cell Biol.* 2010;12(12):1213-1219.

27. Suzuki S, Suzuki N, Mirtsos C, et al. Nur77 as a survival factor in tumor necrosis factor signaling. *Proc Natl Acad Sci USA.* 2003;100(14):8276-8280.

28. Min IM, Pietramaggiori G, Kim FS, Passegué E, Stevenson KE, Wagers AJ. The transcription factor EGR1 controls both the proliferation and localization of hematopoietic stem cells. *Cell Stem Cell.* 2008;2(4):380-391.

29. Passegué E, Wagner EF, Weissman IL. JunB deficiency leads to a myeloproliferative disorder arising from hematopoietic stem cells. *Cell.* 2004;119(3):431-443.

30. Alabert C, Groth A. Chromatin replication and epigenome maintenance. *Nat Rev Mol Cell Biol.* 2012;13(3):153-167.

31. Alabert C, Bukowski-Wills JC, Lee SB, et al. Nascent chromatin capture proteomics determines chromatin dynamics during DNA replication and identifies unknown fork components. *Nat Cell Biol.* 2014;16(3):281-293.

32. Chen C, Liu Y, Liu Y, Zheng P. Mammalian target of rapamycin activation underlies HSC defects in autoimmune disease and inflammation in mice. *J Clin Invest.* 2010;120(11):4091-4101.

33. King KY, Goodell MA. Inflammatory modulation of HSCs: viewing the HSC as a foundation for the immune response. *Nat Rev Immunol.* 2011;11(10):685-692.

34. Yang L, Qian Y, Eksioglu E, Epling-Burnette PK, Wei S. The inflammatory microenvironment in MDS. *Cell Mol Life Sci.* 2015;72(10):1959-1966.

35. Huether R, Dong L, Chen X, et al. The landscape of somatic mutations in epigenetic regulators across 1,000 paediatric cancer genomes. *Nat Commun.* 2014;5(3630):3630.

36. Mets E, Van Peer G, Van der Meulen J, et al. MicroRNA-128-3p is a novel oncomiR targeting PHF6 in T-cell acute lymphoblastic leukemia. *Haematologica.* 2014;99(8):1326-1333.

37. Wendorff AA, Quinn SA, Rashkovan M, et al. Phf6 loss enhances HSC self-renewal driving tumor initiation and leukemia stem cell activity in T-ALL. *Cancer Discov.* 2019;9(3):436-451.